

# Synthesis and functionalization of mucoadhesive mesoporous silica particles containing diphenhydramine for treatment of aphthous ulcers

Azadeh Vaezi Moghaddam<sup>1,2</sup>, Seyed Alireza Mortazavi<sup>1\*</sup>, Farzad Kobarfard<sup>3</sup>, Reza Bafkary<sup>4</sup>, Behzad Darbasizadeh<sup>1</sup>

<sup>1</sup>Department of Pharmaceutics and Pharmaceutical Nanotechnology, School of Pharmacy, Shahid Beheshti University of Medical Sciences, Tehran, Iran

<sup>2</sup>Student Research Committee, Shahid Beheshti University of Medical Sciences, Tehran, Iran

<sup>3</sup>Department of Medicinal Chemistry, School of Pharmacy, Shahid Beheshti University of Medical Sciences, Tehran, Iran

<sup>4</sup>Department of Pharmaceutical Nanotechnology, Faculty of Pharmacy, Tehran University of Medical Sciences, Tehran, Iran

## Article Info



### Article Type:

Original Article

### Article History:

Received: 27 July 2022

Revised: 15 Oct. 2022

Accepted: 19 Nov. 2022

ePublished: 16 July 2023

### Keywords:

Buccal delivery,  
 Mucoadhesive,  
 Mesoporous silica nanoparticles,  
 Oral ulcers

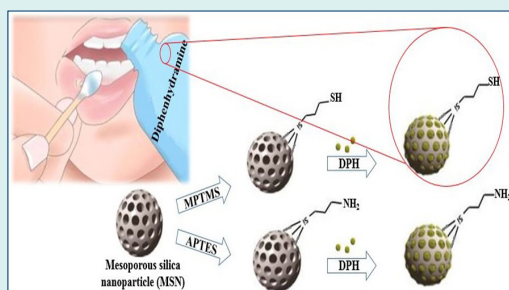
## Abstract

**Introduction:** Medications used to treat oral ulcers include corticosteroids, anesthetics, and antihistamines. These can be used as gels, mouthwashes, pastes, ointments, etc. Diphenhydramine hydrochloride (DPH) has local anesthetic properties that can help treat the aphthae. One of the drawbacks of the delivery to the transmucosal is the quick turnaround time of the gel, a mucous form that is located on the epithelial film surface.

**Methods:** Therefore, it seems that the preparation of a carrier that has the characteristics of adhesive mucus can increase the duration of drug retention on the mucous surface. To solve this problem, mesoporous silica nanoparticles (MSNPs) were synthesized and functionalized with amino and thiol groups and suggested as a system of drug delivery. The properties and structure of MSNPs were investigated by dynamic light scattering (DLS), transmission electron microscopy (TEM), energy-dispersive X-ray spectroscopy (EDS), thermal gravimetric analysis (TGA), Fourier transform infrared spectroscopy (FTIR), and nitrogen adsorption-desorption isotherms (BET).

**Results:** Our outcomes indicated that the average sizes of bare MSNPs (MSN), amino modified MSNPs (MSN-NH<sub>2</sub>), and thiol modified MSNPs (MSN-SH) were obtained to be 611, 655, and 655 nm respectively and the average pore size of MSN, MSN-NH<sub>2</sub>, and MSN-SH were about 2.42 nm, 2.42 nm, and 2.44 nm, respectively, according to the BJH (Barrett-Joyner-Halenda) pore size distribution. The release kinetics and release of DPH from mesoporous silica carriers were evaluated.

**Conclusion:** Eventually, the mucoadhesive study and DPH-loaded particles were investigated. Also, the MSN-SH exhibited a high mucoadhesive capacity for buccal mucosa compared with MSN-NH<sub>2</sub> and MSN.



## Introduction

The most usual damages to the oral mucosa are acute oral ulcers. The mucous membrane of the mouth is prone to painful sores.<sup>1-3</sup> Although acute oral ulcers indicate a very current oral lesion, its definite etiology is indistinct. Multifarious factors, such as local damage, immunodeficiency, infection, systemic diseases, and allergic agents have been noticed in the pathogenesis of acute oral ulcers.<sup>1-5</sup>

Currently, no therapeutic therapy is available, because

the pathogenic factors remain unclear. Therefore, treatment is only symptom therapy to improve and relieve the symptom.<sup>4</sup> Therefore, a numerous variety of medications including antihistamines, corticosteroids, analgesics, antimicrobials, and biologics that improve epithelial repair are prescribed to treat the aphthae.<sup>4</sup> Diphenhydramine hydrochloride (DPH) is an antagonist of histamine which is an ingredient of common cold preparations. Moreover, the local anesthetic properties of DPH could potentially make it an efficient candidate for

\*Corresponding author: Seyed Alireza Mortazavi, Email: [mortazavisar@yahoo.com](mailto:mortazavisar@yahoo.com)



apthae treatment.<sup>6,7</sup> The oral cavity has been considered for delivery of drug because of some advantages like bypassing first-pass effect, ease of administration, and patient compliance.<sup>5</sup> The transmucosal route uses two buccal and sublingual areas for different therapeutic purposes.<sup>8</sup>

Drug delivery to the oral mucosa has limitations, which involves the quick turnaround time of the gel, a mucous form that is located on the epithelial film surface. This quickly removes the medicinal formulations from the oral mucosa.<sup>9</sup> It is proven that the preparation of a carrier that has the characteristics of adhesive mucus can increase the duration of drug retention on the mucous surface.<sup>10</sup> To prepare adhesive mucus carriers, they can be functionalized with different groups, including thiol groups. Thiolated carriers can form strong covalent bonds with mucus glycoproteins.<sup>11,12</sup> In the past years, several nanotechnology-based pharmaceutical carriers such as dendrimers, liposomes, mesoporous silica particles (MSPs), polymeric Particles are used for drug delivery.<sup>13</sup> These carriers can be engineered with functional groups such as hydroxyl, carboxyl, amino, or Sulfhydryl, which leads to adhesion to the mucosa by forming disulfide bridges or hydrogen bonds.<sup>13</sup> For instance, natural bio adhesives such as chitosan can form an electrostatic bond with the negative charge of mucin.<sup>14,15</sup> However, thiolated chitosan demonstration augmented adhesive mucosal effects owing to formation of covalent bond with cysteine-rich domains of mucus glycoproteins. It has been confirmed that non-covalent bonds such as van der Waals forces, hydrogen bonds, and ionic interactions are weaker than covalent bonds.<sup>16,17</sup> Mesoporous silica nanoparticles (MSNPs) have been extensively considered as carriers of drug delivery.<sup>18</sup> MSNPs with unique properties such as particle size adjustment, uniform mesoporous, porous interior space that is suitable for loading drug, a vast area of surface, and easy modifications of surface can be used as a suitable drug carrier.<sup>18,19</sup> However, MSNPs are not suitable adhesives due to their negative surface charge.<sup>20</sup> It is expected that modification of the MSNs surface with various functional groups such as; -NH<sub>2</sub> and -SH could potentially enhance the mucoadhesive property, which could make them efficient drug delivery systems through the mucus.

In this line of study, Wang et al poly (amidoamine) (PAMAM) modified MSNPs for potential bladder cancer therapy. They realized that by raising the number of PAMAM amino groups on the surface of the MSNs, the mucoadhesive capacity is expanded.<sup>20</sup> In another study,  $\beta$ -cyclodextrin functionalized MSPs with hydroxyl, amino, and thiol groups were synthesized. The thiol-functionalized nanoparticles exhibited high mucoadhesive on the urothelium significantly.<sup>13</sup> Mao et al synthesized modified MSNPs with polymer of thiolation and cell-penetrating peptide, which promoted the adhesion to the mucosa and cellular interactions.<sup>21</sup>

In this study, we synthesize functionalized mucoadhesive

MSPs with amino and thiol groups, for the first time to help treating aphthous sores. Also, the duration of adhesive mucosa of bare MSNPs and functionalized MSNPs on the buccal surface for 12 hours was examined and compared. In this study, the release of diphenhydramine from bare MSNPs and functionalized MSNPs particles were investigated. MSNPs and their functionalization aimed to increase the residence time of the mucosa for 12 hours and the controlled release of the drug. The synthesized MSNPs were characterized by Fourier transform infrared spectroscopy (FTIR), energy-dispersive X-ray spectroscopy (EDS), thermal gravimetric analysis (TGA), dynamic light scattering (DLS), Brunauer-Emmett-Teller (BET), X-ray diffraction (XRD), and transmission electron microscopy (TEM).

## Materials and Methods

### Materials

Cetyltrimethylammonium bromide (CTAB), (3-Aminopropyl) triethoxysilane (APTES) as a functionalized group, tetraethyl orthosilicate (TEOS) as a source of silica, (3-mercaptopropyl) trimethoxysilane as a functionalized group, Quinacrine hydrochloride as a fluorescent substance, and DPH were prepared from corporation of Sigma-Aldrich. Solution of phosphate-buffered saline (PBS), Deionized water, Ethanol, and ammonia were used throughout this work that were purchased from Merck Co (Merck, Germany).

### Synthesis of MSNPs

To synthesize MSNPs, we combined 0.3 g CTAB with ammonia (11 mL), ethanol (58 mL), and deionized water (144 mL). Then, the prepared composition was heated up to 60 °C under vigorous stirring for 15 minutes. Subsequently, about 1 mL of TEOS was added drop by drop. It was mixed for 2 hours until particles were formed. Then the filtered formulation was washed, and finally dried under vacuum.<sup>22</sup>

### Functionalization of MSNPs

After MSNPs synthesis, thiol and amino-functionalized MCM-41 were prepared separately by the following method:

MCM-41-thiolated particles were obtained using (3-mercaptopropyl) trimethoxysilane as follows. MSNPs (500 mg) were refluxed with absolute ethanol (30 mL) and 3-mercaptopropyl (5 mL) trimethoxysilane for 24 hours. After the surface modification step, the filtered formulation was washed. CTAB was removed by two stages of reflux. In the first stage, the particles (500 mg) were combined with methanol (100 mL) and Ammonium nitrate (428 mg) for 24 hours at 60 °C. In the second stage, the particles (500 mg) were combined with 37.4% HCl (6 mL) and methanol (100 mL) at 60 °C for 24 hours. The filtered formulation was then washed, and finally dried

under vacuum.<sup>22,23</sup>

Amino-functionalized MCM-41 samples were provided similar to the method described in the thiol-functionalized.

#### Fourier transform infrared analysis

To study the structure and position of silane groups on the external of MSNPs FTIR analysis (WQF-510, Raleigh Optics, China) was used. In FTIR analysis, the samples were dispersed in pellets of KBr and ran versus a pellet of blank KBr background at the wavenumber range of 400-4000  $\text{cm}^{-1}$ .

#### Energy dispersive X-ray spectroscopy

Elemental analyses of freeze-dried NPs were carried out using EDAnalysis (FESEM, TESCAN Company, Czech Republic) attached to SEM (S-4100, Hitachi, Japan).

#### Thermal gravimetric analysis

Freeze-dried nanoparticles were subjected to thermogravimetric analysis by TGA apparatus (TGA 50, Shimadzu Company, Japan). The particles were heated under nitrogen gas at a rate of 10  $^{\circ}\text{C}/\text{min}$  at a temperature of 30-700  $^{\circ}\text{C}$ .

#### Zeta potential and particle size by DLS

By the method of light scattering using the instrument of a Malvern Zetasizer Nano-ZS the mean particle size (z-ave) and polydispersity index (Pdl) of prepared MSNPs were checked. For DLS information, 1 mL of a suitable concentration of each sample was poured into a glass cuvette and the particle size distribution was studied by DLS using a Malvern Zetasizer Nano-ZS appliance (Malvern Instrument, Ltd., Worcestershire, UK). All DLS tests on particles were done at 25  $^{\circ}\text{C}$  and at 173  $^{\circ}$  scattering angle for 3 cycles with an equilibration time of 120 seconds. Zeta-potential values were obtained using a Malvern Zetasizer Nano-ZS at 25  $^{\circ}\text{C}$  in deionized water. Standard deviations were calculated with 20 sub runs. For this reason, sample suspension in deionized water at 0.1 mg/mL concentration was ready.

#### Morphological characterization

The morphology of the MSNPs was investigated by TEM (CM120, Holland). To check the morphology of MSNPs, the solution containing essence was dried on a copper grid with a carbon layer.

#### X-ray crystallography or X-ray diffraction

The crystallinity of the MSNPs was analyzed by diffractometer of X-ray (X'Pert PRO MPD, PANalytical BV, The Netherlands) at 25.0  $^{\circ}\text{C}$ , using Cu K $\alpha$ 1 (40 mA, 40 kV,  $\lambda = 1.54060 \text{ \AA}$ ) radiation over the  $2\theta$  range of 0.6-10 $^{\circ}$ . Peak positions, the corresponding repeat distances, and relative intensities were obtained using the PANalytical X'pert HighScore software with version 3.0.5.

#### Nitrogen adsorption-desorption isotherms

The surface area of the samples was analyzed by physisorption of nitrogen gas at -196.15  $^{\circ}\text{C}$  over a BET (BELSORP MINI II, BEL Company).

#### Determinations of entrapment efficiency and drug loading

First, a solution with a 2.5 mg/mL concentration in a solution of PBS (pH=6.8) was prepared. Next, 10 mg of MSN and modification MSN were poured into the solution and at a temperature of the room stirred for 24 hours to attain the balance condition. Then, the DPH-loaded particles were aggregated by centrifugation and leached with PBS buffer (pH=6.8) solution. The content of DPH loaded into MSNPs was evaluated by alleviating the content of DPH in the aggregated supernatant from the initial content of DPH in the loading solution using a UV-vis spectrophotometer (UV2601 UV/VIS, China) at 220 nm. The drug loading (%DL) and entrapment efficiency (%EE) of diphenhydramine chloride were computed conforming to equations 1 and 2 respectively:

$$\% \text{drug loading} = \frac{\text{Amount of DPH entrapped in MSNPs}}{\text{Total Weight of MSNPs}} \times 100\% \quad (1)$$

$$\% \text{entrapment efficiency} = \frac{\text{Amount of DPH entrapped in MSNPs}}{\text{weight of initial DPH}} \times 100\% \quad (2)$$

#### In vitro release profiles

Formulation powders containing DPH (5 mg) were interspersed in 5 mL of PBS (pH 6.8) in a membrane bag of dialysis (MWCO 12000Da, flat width 43 mm, Length 5 mm, Sigma-Aldrich), and the bags were plunged in 50 mL of PBS (pH 6.8) and stirred at a temperature of 37  $^{\circ}\text{C}$ . The content of DPH released was determined by UV-Vis absorption spectroscopy) at 258 nm.

The drug release curve from the particles was evaluated with the following formulas.

$$\text{Kinetics model of zero-order: } M_0 - M_t = k_0 t \quad (3)$$

Kinetics model of first-order:

$$\text{Log}(100 - M_t) = \text{Log} 100 - k t / 2.303 \quad (4)$$

$$\text{Kinetics model of Higuchi: } M_t = k_H t^{1/2} \quad (5)$$

$$\text{Kinetics of Hixson-Crowell: } (M_0 - M_t)^{1/3} = k_H C t \quad (6)$$

Here  $M_0$  is the primary drug concentration in dilution,  $M_t$  is the drug concentration released at time  $t$ , and  $k_0$ ,  $k_1$ ,  $k_H C$ , and  $k_H$  are the drug release rate constants of zero-order, first-order, Hixson.Crowell, and Higuchi, kinetics models, respectively.

$$\text{Model of Korsmeyer - Peppas: } M_t/M_{\infty} = k t^{1/2} \quad (7)$$

$M_t/M_{\infty}$  in the formula represents the drug released at time  $t$ ,  $k$  is the constant of rate, and  $n$  is the power of release. Model of Korsmeyer-Peppas is a pattern portraying the release of drug from matrixes of polymer. In the model of Korsmeyer-Peppas, 60% of the initial drug released is fitted to the equation which  $k$  is the constant of release

rate and  $n$  is the power of release. The  $n$  content is utilized to realize the mechanism of release. If the  $n$  content is  $0.45 < n < 1$  or  $n \leq 0.45$  the mechanism of release would follow the non-Fickian diffusion or Fickian diffusion, respectively. If  $n = 1$ , the release of drug follows zero-order kinetics or Case-II transport. For  $n > 1$ , the mechanism of the drug release is Case-II transport.

#### **Buccal tissue preparation and mucoadhesive study**

Mucoadhesive attributes of the functionalized silica nanoparticles were determined according to the previously described procedure.<sup>9,24,25</sup> Quinacrine used as a probe of fluorescence was caught in the MSPs. Buccal tissue, freshly excised from bovine, was obtained from a slaughterhouse. Surplus and extra tissue on the buccal were eliminated, and the buccal was sliced to size almost 4 cm<sup>2</sup>, mucous tissue obtained from the slaughterhouse was placed on a slope with an angle of approximately 45 degrees. The mucosa was incubated with 90  $\mu$ L of Quinacrine-loaded bare MSNPs (MSN), amino modified MSNPs (MSN-NH<sub>2</sub>), and thiol modified MSNPs (MSN-SH) for 2 hours at 37 °C.<sup>13,26</sup> Then, buccal tissue was slowly and continuously washed for 6 hours with PBS pH 6.8 at a rate of 3 mL/h.<sup>9</sup> Sampling was done once every hour. The number of particles in the sample was identified by cyotation imaging reader (Biotek, U.S) and calculated using the formula.

#### **Statistical analysis**

Using IBM SPSS Statistics version 21.0 software, the data of this research was analyzed statistically. One-way ANOVA and paired-sample  $t$  test analyses were used to assess whether the values were statistically different.  $P$  values of  $\leq 0.05$  were noticed as significant differences.

## **Results**

#### **Synthesis and characterization of MSNPs**

Fig. S1A and S1B represent the XRD and EDS spectra

of the synthesized MSNPs (See Supplementary file 1). The strong peak (100) in Fig. S1A, sharply indicates the existence of MCM-41 structure and also two other peaks (110) and (200) which are weak could be attributed to the 2-D hexagonal lattice (P6mm) group of space, to show a hexagonal mesostructured substance with a high degree of long-range ordering of the structure. Peak broadening was generally seen in structures with wormhole arrays and the move towards smaller angles reflect a deflection in packing of the pores with regards to ordered MCM.<sup>13,27</sup> The EDX spectra of the MSN, MSN-NH<sub>2</sub>, and MSN-SH are shown in Fig. S1B. As shown in Fig. S1B the EDX spectrum of MSN reveals the presence of carbon, nitrogen, oxygen, and silica. High levels of C and N atoms were due to the presence of CTAB, which were utilized for synthesis (Table 1).

However, after the removal of CTAB, only the spectra of silica and oxygen elements were seen, which proves the complete removal of CTAB. EDX analysis of the MSN-SH sample showed spectra related to silica, sulfur, carbon, and oxygen. The presence of a sulfur spectrum indicated successful functionalization of MSN with -SH moiety. Also, in the MSN-NH<sub>2</sub> sample nitrogen spectrum was observed, which proved amine surface modification. According to the above-mentioned explanations, it was demonstrated that MSN was successfully synthesized and then functionalized with thiol and amine groups.

#### **Morphology observation**

TEM micrographs of synthesized MSN and MSN-SH in Fig. 1 reveal the organization of nanoparticles with spherical morphology distribution and the channels of mesoporous silica. Fig. 1A and 1B regarding. Also, Fig. 1D shows mesoporous silica without surfactant, which has parallel and direct channels.

#### **FT-IR analysis**

Spectroscopy of FTIR was applied to analyze the potential

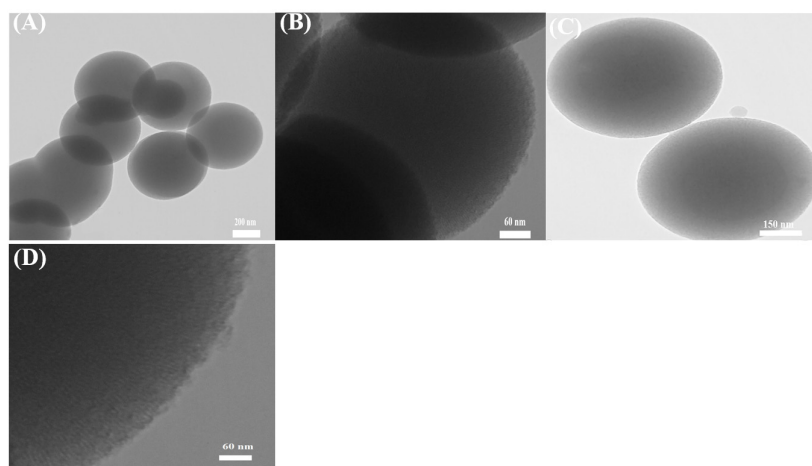


**Fig. 1.** TEM micrographs of (A), (B) and (D) MSN, (C) MSN-SH without CTAB.

**Table 1.** The amount of elements in mesoporous silica samples

Particles	Atomic percentage (%)				
	C	N	O	Si	S
MSN with CTAB	45.92	10.22	31.70	12.16	0.00
MSN without CTAB	0.00	0.00	74.95	25.05	0.00
MSN-NH <sub>2</sub>	27.42	2.08	45.07	25.43	0.00
MSN-SH	36.14	0.00	41.64	17.65	4.57

structural changes which might occur between the MSN and functionalized MSN. Nonfunctionalized MSN spectra of FTIR with and without CTAB are shown in Fig. 2A and 2B, respectively. After CTAB was removed from the mesoporous silica channels, they were removed from the spectrum at 2855 and 2926  $\text{cm}^{-1}$  frequencies.<sup>20,28</sup> Spectra of MSN, MSN-NH<sub>2</sub>, MSN-SH exhibited IR peaks at the bands attributed to symmetric stretching of Si-O-Si at 796  $\text{cm}^{-1}$ , Si-O-Si asymmetric stretching at 1067  $\text{cm}^{-1}$ , -OH bending vibration of the physisorbed water molecules by the silica materials at 1633  $\text{cm}^{-1}$  and Si-OH stretching at 3290  $\text{cm}^{-1}$ .<sup>29</sup>

After modification with APTES, the structure of the MSN was preserved without significant change in the framework. The existence of amino group on the surface of particles was established by the apparition of the peaks at 2911  $\text{cm}^{-1}$  and 1578  $\text{cm}^{-1}$  which related to the methylene (C-H) and N-H stretch vibrations of APTES being connected to the MSN framework (Fig. 2D).<sup>20,28,30</sup> The MSNPs-SH has a weak stretching spectrum at the frequency of 2550  $\text{cm}^{-1}$ , which indicates the presence of the thiol group and S-H bond as well.<sup>13</sup>

#### Zeta potential and particle size by DLS

Zeta potential and particle size of MSN and the modification MSN were checked by DLS and displayed in Fig. 3. According to the outcomes, the average sizes of

MSN, MSN-NH<sub>2</sub>, MSN-SH nanoparticles were measured  $611 \pm 0.007$ ,  $655 \pm 0.006$ , and  $655 \pm 0.005$  nm respectively (Fig. 3B).<sup>31</sup> PDI of MSN, MSN-NH<sub>2</sub>, MSN-SH nanoparticles were found to be  $0.292 \pm 0.007$ ,  $0.336 \pm 0.006$ , and  $0.336 \pm 0.005$  nm respectively. Fig. 3A displays the zeta potential of MSN, MSN-NH<sub>2</sub>, and MSN-SH nanoparticles. After surfactant removal the zeta potential of MSN was observed to become negative  $-19.9 \pm 1.1$  mV, which indicates the elimination of surfactant and hydroxyl groups on the surface. As shown in Fig. 3A, the zeta potential of amino-functionalization of MSN increased the potential from  $-19.9 \pm 1.1$  mV to  $+29.8 \pm 1.7$  mV in deionized water at pH=6.5 and temperature of 37 °C, which shows the functionalization of particles with amine groups.<sup>29</sup> Moreover, after presenting -SH moiety on the surface of the MSNs, the potential was decreased from  $-19.9 \pm 1.1$  mV to  $-22.4 \pm 1.5$  mV.<sup>29</sup>

Based on the results, it is expected that the MSN nanoparticles were successfully functionalized with amine and thiol groups, which is in agreement with the EDX and FTIR results.

#### Thermal gravimetric analysis

Analysis of TGA was performed on all three formulations MSN, MSN-NH<sub>2</sub>, and MSN-SH to confirm surfactant removal and surface modification. From the TGA curve (Fig. 4), after the completion of the TGA analysis all of the

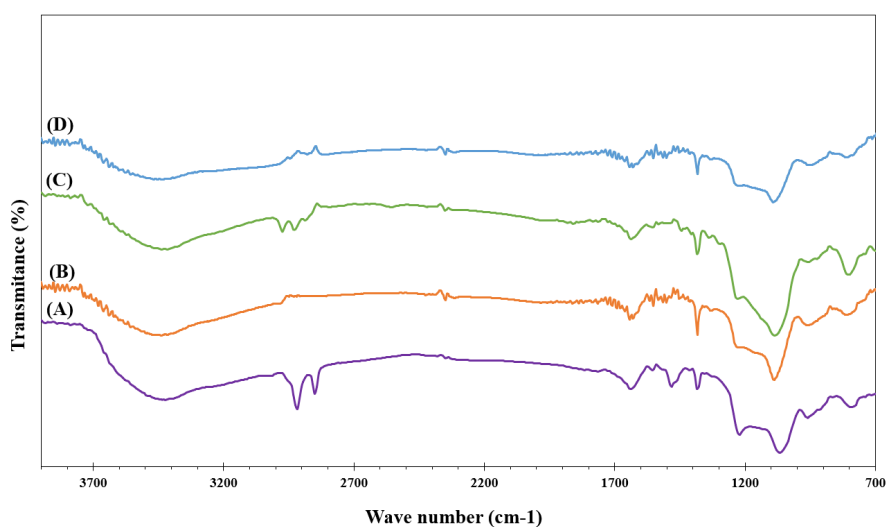


**Fig. 2.** The FTIR spectra of (A) MSN with CTAB (B) MSN without CTAB (C) MSN-SH without CTAB (D) MSN-NH<sub>2</sub> without CTAB.

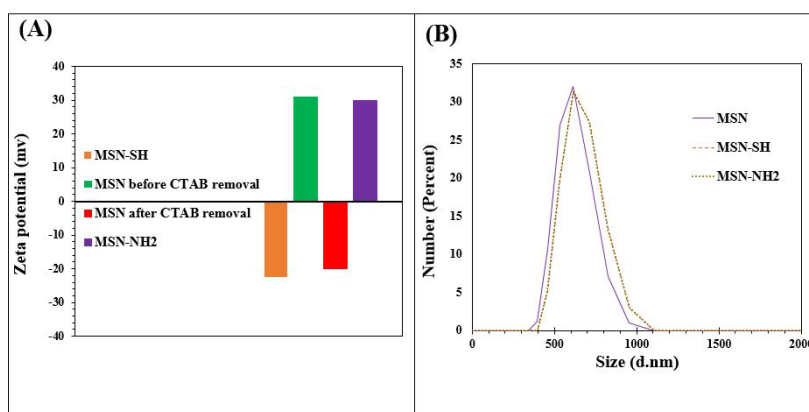


**Fig. 3.** (A) Zeta potential results of samples MSN, MSN-SH, and MSN- NH2 before and after CTAB removal, (B) Size distribution study of MSN, MSN-SH, and MSN-NH2.

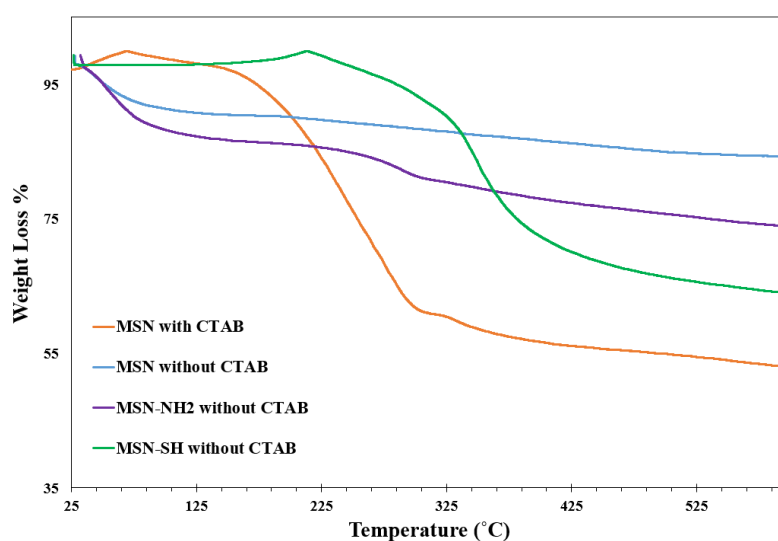


**Fig. 4.** TGA analysis of MSN without CTAB, MSN with CTAB, MSN-NH2 without CTAB, and MSN-SH without CTAB.

particles of the sample have a weight loss due to the loss of water that was physically on the surface of the particles at a temperature of 150 °C.<sup>29</sup> The whole weight reduction of MSN, MSN-NH2, and MSN-SH containing CTAB is 45%, 27%, and 36% respectively and the total weight loss of MSN, MSN-NH2, and MSN-SH without CTAB was 12.5%, 22%, and 27% respectively.

#### Nitrogen adsorption-desorption isotherms

According to the results of N<sub>2</sub> adsorption isotherms, all three formulas correspond to type-IV isotherms,<sup>32</sup>

thus, demonstrating that the particles attracted the same mesoporous channels and narrow pore size dispersion.<sup>32,33</sup> The BJH (Barrett-Joyner-Halenda) pore diameter, BET surface area and pore volumes are written in Table 2 and Fig. 5. The surface areas of MSN, MSN-NH2, and MSN-SH were computed to be in order 358.41 m<sup>2</sup> g<sup>-1</sup>, 371.92 m<sup>2</sup> g<sup>-1</sup>, and 463.61 m<sup>2</sup> g<sup>-1</sup> in order.

The average pore sizes of MSN, MSN-NH2, and MSN-SH were about 2.42 nm, 2.42 nm, and 2.44 nm, respectively, according to the BJH pore size distribution.

This information demonstrates that the MSN, MSN-

**Table 2.** BET data of the synthesized particles

Particles	Pore volume (cm <sup>3</sup> /g)	Specific surface area (m <sup>2</sup> /g)	Pore diameter ( nm)
MSN with CTAB	0.10	49.87	2.42
MSN without CTAB	0.24	332.04	2.42
MSN-SH without CTAB	0.34	600.08	2.44
MSN-NH2 without CTAB	0.27	543.97	2.42

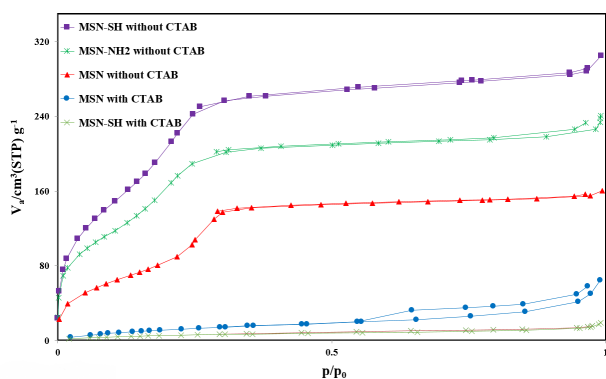


**Fig. 5.** Nitrogen adsorption-desorption isotherms of MSN-SH with CTAB, MSN with CTAB, MSN without CTAB, MSN-NH<sub>2</sub> without CTAB, and MSN-SH without CTAB.

SH, and MSN-NH<sub>2</sub> were well prepared as standard Mesoporous silica. As shown in the table, the specific surface area and the pore volume have increased after the removal of CTAB, which indicates the removal of the CTAB.

**Determinations of drug loading and entrapment efficiency**

After successful synthesis of MSN, MSN-NH<sub>2</sub>, and MSN-SH, DPH was used with anesthetic effect to treat the pest for drug delivery. MSN, MSN-NH<sub>2</sub>, and MSN-SH were immersed in DPH solutions in various ratios of 1: 1, 1: 2, and 2: 1 for 24 hours. Subsequently, the solutions were centrifuged and the remained drug in the supernatant was determined to find out the encapsulated drug in the MSNs. The amount of loaded DPH into the MSNs was calculated via EE and DL equations in section 2.11.

DPH and MSNs were mixed at various ratios, but the highest percentage of EE and DL were related to the ratio of 1: 1, and the outcomes are presented in Table 3.

The results show that bare MSN loaded about 39.02±1.6% of DPH after 24 hours. However, the functionalization on the surface of bare MSN had decreased the amount of DPH loaded. The DL percentages were 38.27±1.7% and 37.50±1.5% for MSN-NH<sub>2</sub> and MSN-SH, respectively.

**Study of in vitro release and kinetics of release**

The total amount of DPH released from MSN, MSN-SH, and MSPs-NH<sub>2</sub> over 48 hours in solution of phosphate buffer (pH 6.8) was within the range of 60%-64%. As illustrated in Fig. 6, the release of DPH from MSN, MSN-SH, and MSN-NH<sub>2</sub> represented a biphasic manner so that in the first hour, the release of the drug is in the form of

**Table 3.** Percentage of EE and DL calculated particles

Particles	Carrier: drug	EE	DL
MSN	1:1	64.0±1.7%	39.02±1.6%
MSN-NH <sub>2</sub>	1:1	62.0±1.8%	38.27±1.7%
MSN- SH	1:1	60.0±1.7%	37.50±1.5%

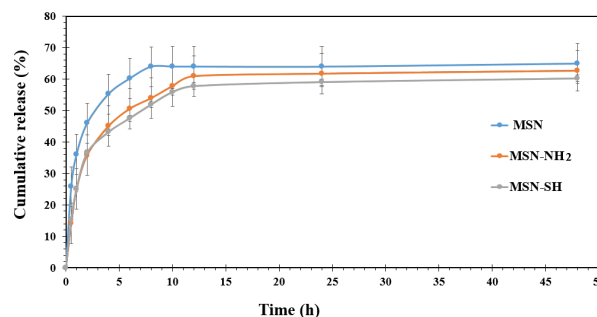


**Fig. 6.** In vitro DPH release profiles from MSN, MSN-NH<sub>2</sub>, and MSN-SH in PBS (pH 6.8) at 37 °C (n = 3).

a burst, and then the release is done slowly for 48 hours. As shown in Fig. 6, after 6 hours, the percentage of drug released of bare MSN sample was 60.46%, while, the functionalized MSN-NH<sub>2</sub> and MSN-SH samples released 50.5% and 47.5% of the loaded drug, respectively. The outcomes exhibited that the functionalization of MSPs slows down the release of the drug.

To perusal, the release kinetics, the coefficient (R<sup>2</sup>) is accounted as a single and segmental kinetic model for each release profile. According to the outcomes shown in Table 4, whole kinetic of single models values of R<sup>2</sup> are fewer than models of segmental, so the interpretation of the results and the selection of the release kinetics is based on the segmental models. Through matching the segmental kinetic models, results of DPH release from MSN, MSN-NH<sub>2</sub>, and MSN-SH were fitted with Higuchi Model.<sup>34</sup> The release type of DPH drug was investigated by model of Korsmeyer-Peppas, and resulted obtained from them were displayed in Table 4.<sup>34</sup>

**Mucoadhesive study**

The adhesive mucosa test results of MSN, MSN-SH, and MSN-NH<sub>2</sub> are displayed in Fig. 7 and Fig. 8. As it could be observed, the percentage of particles remaining on the mucosal tissue after 6 hours was found to be 91%, 60.9%, and 30.8% for MSN-SH, MSN-NH<sub>2</sub>, and MSN respectively. In addition, after 12 hours, the remaining particles were 80%, 50%, and 18% respectively. Silica particles possess many hydroxyl groups on their surface, which can cause hydrogen bond formation with mucin.<sup>35</sup>

The outcomes displayed that the adhesion efficiency of the MSN-SH sample to mucosa was stronger than the two other samples. Most probably, this was because thiol functional groups are located on the surface of the particles which allows the formation of stable covalent bonds with cysteine subdomains of mucosal glycoproteins.<sup>17, 36</sup>

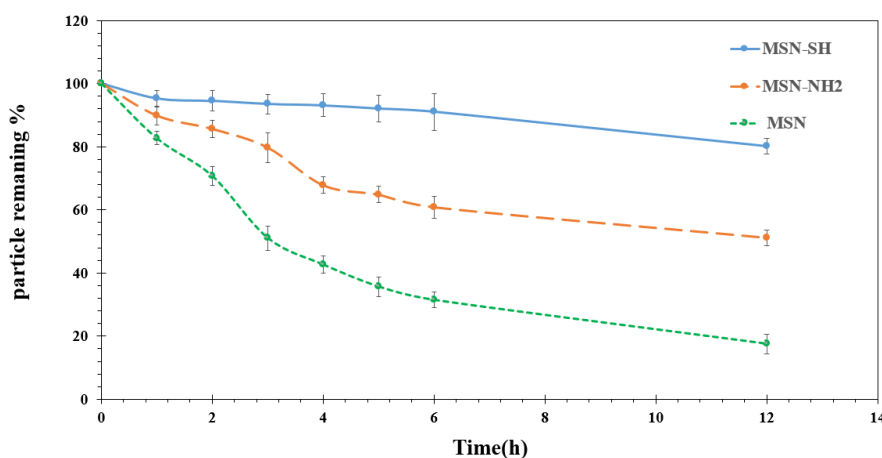
The outcomes displayed that the adhesion efficiency of the MSN-SH sample to mucosa was stronger than the two other samples. Most probably, this was due to the presence of thiol groups on the surface of mesoporous silica which allows the formation of stable covalent bonds with cysteine subdomains of mucosal glycoproteins.<sup>22,37</sup>

**Table 4.** Kinetic models of DPH released from the MSN, MSN- SH, and MSN-NH2

Formulation	Time (h)	Zero order		First order		Higuchi		Fickian-spherical		Korsmeyer-Peppas		
		$K_0$ ( $\mu\text{g}/\text{cm}^2/\text{h}$ )	$R^2$	$k^{-1}(\text{h}^{-1})$	$R^2$	$K_H$ ( $\mu\text{g}/\text{cm}^2/\text{h}^{0.5}$ )	$R^2$	$K$ ( $\mu\text{g}/\text{cm}^2/\text{h}^{0.43}$ )	$R^2$	$k_{kp}$	$n$	$R^2$
MSN	Total (0-48)	0.53	0.31	0.01	0.27	6.67	0.68	0.01	0.27	37.13	0.2	0.81
	1st stage (0-8)	4.64	0.87	0.05	0.78	17.33	0.95	21.72	0.96	34.55	0.31	0.97
	2st stage (8-48)	0.03	0.89	0.0002	0.89	0.25	0.82	0.36	0.81	62.64	0.008	0.736
MSN-NH2	Total (0-48)	0.74	0.42	0.04	0.71	7.21	0.67	10.21	0.71	24.92	0.32	0.84
	1st stage (0-12)	3.57	0.85	0.04	0.70	15.87	0.95	20.34	0.96	22.9	0.43	0.94
	2st stage (12-48)	0.05	0.96	0.0003	0.95	0.53	0.98	0.77	0.99	57.66	0.022	0.99
MSN-SH	Total (0-48)	0.69	0.43	0.01	0.32	5.45	0.55	9.40	0.72	25.41	0.29	0.85
	1st stage (0-12)	3.26	0.85	0.04	0.71	14.46	0.94	18.52	0.95	23.44	0.39	0.95
	2st stage (12-48)	0.06	0.98	0.0005	0.97	0.71	0.99	1.03	0.99	53.64	0.030	0.99

TEM micrographs, shows that the particles size varies from 600-700 nm, and also it was observed that the pore exhibits a worm-like shape. TEM of MSN-SH in Fig. 1C shows that particle functionalization has reduced the resolution of the channels. So, it can be seen, the length and pore size of MSN-SH are so similar to the length and pore size of MSN and they have maintained their tubular structure. The FTIR spectroscopy was applied to analyze the potential structural changes which might occur between the MSN and functionalized MSN. Successful surface modification of MSN with the thiol group was proved by the emergence of a new weak signal at  $2550\text{ cm}^{-1}$  of S-H stretching (Fig. 2C).<sup>29</sup> According to the outcomes of DLS, the average size of the MSN nanoparticles was enhanced slightly after modification.<sup>31</sup> Möller et al perceived that even with a considerable degree of molecular modification it is feasible to acquire nanoparticles with large surface areas and pore volumes. In TGA analysis this difference in weight reduction is due to the presence of the organic combination CTAB and may indicate the elimination of CTAB from MSNPs.<sup>38</sup> It can be seen that the thermal

disintegration of the organic functional groups attached to the surface of the nanoparticles happened in the period of temperature among 150 and  $625\text{ }^\circ\text{C}$ . As compared to bare MSN, MSN-NH2 showed about 22% weight reduction at around  $550\text{ }^\circ\text{C}$  as a result of decomposition of the amine group. Also, the total weight loss of MSN-SH at  $300\text{ }^\circ\text{C}$  is about 27%, which is more than that of bare MSN, which is due to the decomposition of thiol groups in MSN-SH.<sup>29,39</sup> In the loading study, MSN loaded the highest amount of drug due to better interaction i.e. hydrogen bonding between the hydroxyl group of MSN and DPH. DPH has a tertiary ( $3^\circ$ ) amine that forms a weak hydrogen bond. Moreover, MSN-NH2 develops repulsive interaction with the DPH, thus reducing the load compared to MSN. For the case of MSN-SH, the Sulphur does not have the ability to form hydrogen bonds so it has the lowest DL percentage. Based on the information obtained, it was found that the content of the drug-loaded into the mesoporous materials depends on the type of functional groups joined onto the MSNPs framework and the strong connection between the functional groups on the surface of silica and the drug

**Fig. 7.** Mucoadhesive study and photos from MSN, MSN- SH, and MSN-NH2 on Bovine buccal mucosa at  $37\text{ }^\circ\text{C}$  ( $n = 3$ ).

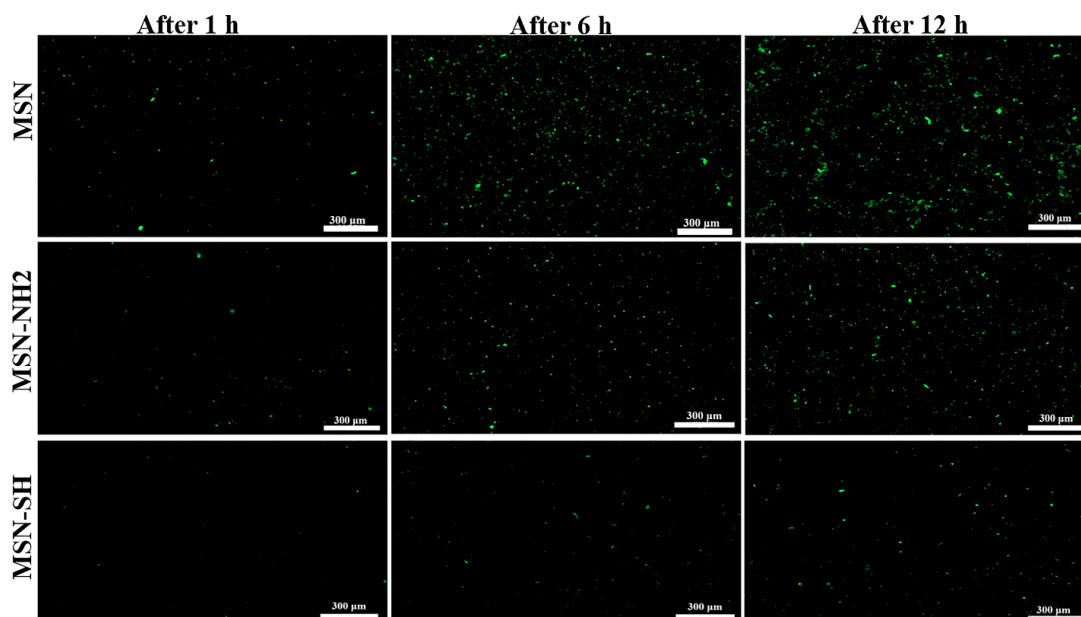


Fig. 8. Mucoadhesive study photos from MSN, MSN- SH, and MSN-NH2 on Bovine buccal mucosa at 37 °C (n = 3).

molecules. Two models of release kinetics are explained below.

#### Model of Higuchi

The model of Higuchi expresses the %release against square root of the time-dependent process based on diffusion of Fickian. Based on this pattern release mechanism of the drug covers concurrent penetration of PBS into the pores, diffusion of these molecules from the pores, and dissolution of the drug molecules. The release mechanism of DPH is best presented by this model with high correlation coefficient and high linearity. This shows that the DPH release follows the mechanism of Fickian diffusion, also a more ordered release profile, which was obtained in cases of MSN, MSN-SH, and MSN-NH2.

#### Model of Korsmeyer–Peppas

This model engendered an experimental equation to examine both non-Fickian and Fickian release of drugs.  $M_t/M_\infty = Kt^n$  is the experimental power that demonstrates the type of release mechanism, wherever  $n = 1.0, 0.5,$  and  $0$  portended First-order, Higuchi, and zero order models respectively.<sup>40</sup> The DPH mechanism of release is best presented by this model with high correlation coefficient and high linearity. The drug release mechanism of all three samples is non-swelling matrix-diffusion due to  $n < 0.5$ .<sup>40</sup> In some studies, it has been seen that drug release from MSPs is in two stages.<sup>18</sup> Xue et al have observed that the two-step drug release is due to the physical and chemical binding of the drug to mesoporous silica. The burst release of the drug is due to the physical connection of the drug with the MSPs. Also, the slower release is due to the chemical binding of the drug, such as hydrogen bonding with the silanol groups

of the MSPs.<sup>41</sup> The zeta potential of all three particles was checked by the DLS device. Zeta potential shows the surface charge of particles. The zeta potential of MSN, MSN-NH2, and MSN-SH before removing CTAB is  $31 \pm 1.7$  mV,  $37 \pm 1.1$  mV, and  $37 \pm 1.5$  mV, respectively. The surface charge of all the particles before removing the surfactant is positive due to the presence of CTAB on their surface. Also the zeta potentials of MSN, MSN-NH2, and MSN-SH after removing CTAB are  $-19.9 \pm 1.1$  mV,  $+29.8 \pm 1.7$ , and  $-22.4 \pm 1.5$  mV respectively. In general, MSN and the modification MSN have decreased their zeta potential after removing the surfactant.<sup>29</sup> In mucoadhesive study, MSN-NH2 possesses a positive charge due to the presence of the amino groups on its surface, which causes the formation of the electrostatic interaction among the mucin sialic groups and amino groups.<sup>42,43</sup> In a 2017 study by Suksiriworapong et al, the researchers studied mucosal drug delivery for the treatment of *Candida albicans* with itraconazole loaded into tubular micelles (TPGS-Cys). The micelles were made of different ratios of TPGS-Cys and TPGS (0: 10, 3: 7, 5: 5, 7: 3, 10: 0) and their size was about 8-10 nm with a spherical shape. They have reported that micelles with TPGS-Cys/TPGS ratios of 0:10 and 3:7 demonstrated good adhesive mucosal properties so that the adhesive duration to the mucosa was twice as long as when TPGS micelles were used alone.<sup>9</sup> Putting all together, it can be concluded that surface modification of the MSNs could increase their mucoadhesive properties which would lead to enhancing their efficiency for drug delivery purposes.

#### Conclusion

In this work, MSN, MSN-NH2, and MSN-SH were synthesized and the effects of their adhesive mucosa were

## Research Highlights

### What is the current knowledge?

- ✓ MSPs are used as drug delivery carriers due to many advantages such as high surface area, easy functionalization, and high loading.
- ✓ Functional groups such as carboxyl, hydroxyl, amino, and Sulfhydryl can bind to the mucus and improve the adhesive effect of the mucus.
- ✓ Thiol functional group can form a disulfide bond with mucus.

### What is new here?

- ✓ MSPs were functionalized with (3-Aminopropyl) triethoxysilane and (3-Mercaptopropyl) trimethoxysilane for the first use in the treatment of aphthous ulcers.
- ✓ The retention time of functionalized particles on the oral mucosa was compared.
- ✓ MSN-SH had the longest persistence on the oral mucosa.

compared and the best particle in terms of the strength of the adhesive mucosa was selected as a mucoadhesive system of drug delivery for the treatment of aphthous ulcer. By optimizing the synthesis conditions (temperature, time, and rotation speed), the average particle size of all three formulations MSN, MSN-NH<sub>2</sub>, and MSN-SH was measured by DLS and the results are 611 nm, 655 nm, and 655 nm respectively. The MSN-SH exhibited a high mucoadhesive capacity for buccal mucosa compared with MSN-NH<sub>2</sub> and MSN because of the formation of a strong covalent bond of thiol group and mucin glycoproteins in mucus. The release of DPH from MSN, MSN-SH, and MSN-NH<sub>2</sub> were biphasic. By comparing the release profiles MSN, MSN-SH, and MSN-NH<sub>2</sub> we found out that the functionalization of silica nanoparticles slows down the drug release process. This study showed that MSN-SH can be used as system of drug delivery to the oral mucosa to treat the aphthae due to its good mucoadhesive and controlled release of DPH.

### Acknowledgment

The authors appreciate SBMU for the pecuniary and instrumental support of this study.

### Authors Contribution

**Conceptualization:** Azadeh Vaezi Moghaddam.

**Data curation:** Azadeh Vaezi Moghaddam.

**Formal analysis:** Azadeh Vaezi Moghaddam.

**Investigation:** Azadeh Vaezi Moghaddam.

**Methodology:** Azadeh Vaezi Moghaddam.

**Project administration:** Azadeh Vaezi Moghaddam, Seyed Alireza Mortazavi.

**Resources:** Azadeh Vaezi Moghaddam.

**Software:** Azadeh Vaezi Moghaddam, Farzad Kobarfard.

**Supervision:** Seyed Alireza Mortazavi.

**Validation:** Azadeh Vaezi Moghaddam.

**Visualization:** Azadeh Vaezi Moghaddam, Reza Bafkary.

**Writing—original draft:** Azadeh Vaezi Moghaddam.

**Writing—review editing:** Azadeh Vaezi Moghaddam, Behzad Darbasizadeh.

### Competing Interests

This study has not received financial support from any specific organization and has no conflict of interest with this publication.

### Ethical Statement

None to be declared.

### Funding

This manuscript was supported by a Shahid Beheshti University of Medical Sciences.

### Supplementary Materials

Supplementary file 1 contains Fig. S1.

### References

1. Bruce A, Rogers R. Acute oral ulcers. *Dermatol Clin* **2003**; 21: 1-15. [https://doi.org/10.1016/S0733-8635\(02\)00064-5](https://doi.org/10.1016/S0733-8635(02)00064-5)
2. Lehman J, Rogers R. Acute oral ulcers. *Clin Dermatol* **2016**; 34: 470-4. <https://doi.org/10.1016/J.CLINDERMATOL.2016.02.019>
3. Baccaglini L, Lalla R, Bruce A, Sartori-Valinotti J, Latortue M, Carrozzo M, et al. Urban legends: recurrent aphthous stomatitis. *J Oral Dis* **2011**; 17: 755-70. <https://doi.org/10.1111/J.1601-0825.2011.01840.X>
4. Belenguier-Guallar I, Jiménez-Soriano Y, Claramunt-Lozano A. Treatment of recurrent aphthous stomatitis. A literature review. *J Clin Exp Dent* **2014**; 6: e168. <https://doi.org/10.4317/JCED.51401>
5. Liu C, Zhou Z, Liu G, Wang Q, Chen J, Wang L, et al. Efficacy and safety of dexamethasone ointment on recurrent aphthous ulceration. *Am J Med* **2012**; 125: 292-301. <https://doi.org/10.1016/J.AMJMED.2011.09.011>
6. Pollack CV, Swindle GM. Use of diphenhydramine for local anesthesia in "caine"-sensitive patients. *J Emerg Med* **1989**; 7: 611-4. [https://doi.org/10.1016/0736-4679\(89\)90006-1](https://doi.org/10.1016/0736-4679(89)90006-1)
7. Ship II, Williams AF, Osheroff BJ. Development and clinical investigation of a new oral surface anesthetic for acute and chronic oral lesions. *Oral Surg Oral Med Oral Pathol* **1960**; 13: 630-6. [https://doi.org/10.1016/0030-4220\(60\)90496-5](https://doi.org/10.1016/0030-4220(60)90496-5)
8. Rossi S, Sandri G, Caramella C. Buccal drug delivery: A challenge already won? *Drug Discov Today Technol* **2005**; 2: 59-65. <https://doi.org/10.1016/J.DDTEC.2005.05.018>
9. Suksiriworapong J, Mingkwan T, Chantasart D. Enhanced transmucosal delivery of itraconazole by thiolated D- $\alpha$ -tocopheryl poly(ethylene glycol) 1000 succinate micelles for the treatment of *Candida albicans*. *Eur J Pharm Biopharm* **2017**; 120: 107-15. <https://doi.org/10.1016/J.EJPB.2017.08.012>
10. Kast C, Guggi D, Langoth N, Bernkop-Schnürch A. Development and in vivo evaluation of an oral delivery system for low molecular weight heparin based on thiolated polycarbophil. *Pharm Res* **2003**; 20: 931-6. <https://doi.org/10.1023/A:1023803706746>
11. Bernkop-Schnürch A, Kast C, Guggi D. Permeation enhancing polymers in oral delivery of hydrophilic macromolecules: thiomers/GSH systems. *J Control Release* **2003**; 93: 95-103. <https://doi.org/10.1016/J.JCONREL.2003.05.001>
12. Clausen A, Kast C, Bernkop-Schnürch A. The role of glutathione in the permeation enhancing effect of thiolated polymers. *Pharm Res* **2002**; 19: 602-8. <https://doi.org/10.1023/A:1015345827091>
13. Zhang Q, Neoh K, Xu L, Lu S, Kang E, Mahendran R, et al. Functionalized mesoporous silica nanoparticles with mucoadhesive and sustained drug release properties for potential bladder cancer therapy. *Langmuir* **2014**; 30: 6151-61. <https://doi.org/10.1021/LA500746E>
14. Sogias I, Williams A, Khutoryanskiy V. Why is chitosan mucoadhesive? *Biomacromolecules* **2008**; 9: 1837-42. <https://doi.org/10.1021/BM800276D>
15. Xu J, Soliman G, Barralet J, Cerruti M. Mollusk glue inspired mucoadhesives for biomedical applications. *Langmuir* **2012**; 28: 14010-7. <https://doi.org/10.1021/LA3025414>
16. Bravo-Osuna I, Vauthier C, Farabollini A, Palmieri G, Ponchel G. Mucoadhesion mechanism of chitosan and thiolated

- chitosan-poly(isobutyl cyanoacrylate) core-shell nanoparticles. *Biomaterials* **2007**; 28: 2233-43. <https://doi.org/10.1016/J.BIOMATERIALS.2007.01.005>
17. Yin L, Ding J, He C, Cui L, Tang C, Yin C. Drug permeability and mucoadhesion properties of thiolated trimethyl chitosan nanoparticles in oral insulin delivery. *Biomaterials* **2009**; 30: 5691-700. <https://doi.org/10.1016/J.BIOMATERIALS.2009.06.055>
  18. McCarthy C, Ahern R, Dontireddy R, Ryan K, Crean A. Mesoporous silica formulation strategies for drug dissolution enhancement: a review. *Expert Opin Drug Deliv* **2016**; 13: 93-108. <https://doi.org/10.1517/17425247.2016.1100165>
  19. Chen Y, Chen H, Shi J. In Vivo Bio-Safety Evaluations and Diagnostic/Therapeutic Applications of Chemically Designed Mesoporous Silica Nanoparticles. *Adv Mater* **2013**; 25: 3144-76. <https://doi.org/10.1002/ADMA.201205292>
  20. Wang B, Zhang K, Wang J, Zhao R, Zhang Q, Kong X. Poly(amidoamine)-modified mesoporous silica nanoparticles as a mucoadhesive drug delivery system for potential bladder cancer therapy. *Colloids Surf B Biointerfaces* **2020**; 189: 110832-. <https://doi.org/10.1016/J.COLSURFB.2020.110832>
  21. Mao Y, Feng S, Zhang X, Zhao Q, Fang Y, Wang S. Thiolated polymer and Cell-Penetrating Peptide dual-surface functionalization of mesoporous silicon nanoparticles to overcome intestinal barriers. *J Drug Deliv Sci Technol* **2019**; 53: 101184-. <https://doi.org/10.1016/J.JDDST.2019.101184>
  22. Manzano M, Aina V, Areán CO, Balas F, Cauda V, Colilla M, et al. Studies on MCM-41 mesoporous silica for drug delivery: Effect of particle morphology and amine functionalization. *Chem Eng J* **2008**; 137: 30-7. <https://doi.org/10.1016/J.CEJ.2007.07.078>
  23. Luo G-F, Chen W-H, Liu Y, Lei Q, Zhuo R-X, Zhang X-Z. Multifunctional enveloped mesoporous silica nanoparticles for subcellular co-delivery of drug and therapeutic peptide. *Sci Rep* **2014**; 4: 6064.
  24. Krauland A, Bernkop-Schnürch A. Thiomers: development and in vitro evaluation of a peroral microparticulate peptide delivery system. *Eur J Pharm Biopharm* **2004**; 57: 181-7. <https://doi.org/10.1016/J.EJPB.2003.09.011>
  25. Yuan Q, Fu Y, Kao WJ, Janigro D, Yang H. Transbuccal Delivery of CNS Therapeutic Nanoparticles: Synthesis, Characterization, and In Vitro Permeation Studies. *ACS Chem Neurosci* **2011**; 2: 676-. <https://doi.org/10.1021/CN200078M>
  26. Suksiriworapong J, Mingkwan T, Chantasart D. Enhanced transmucosal delivery of itraconazole by thiolated d- $\alpha$ -tocopheryl poly(ethylene glycol) 1000 succinate micelles for the treatment of *Candida albicans*. *Eur J Pharm Biopharm* **2017**; 120: 107-15. <https://doi.org/10.1016/J.EJPB.2017.08.012>
  27. Möller K, Kobler J, Bein T. Colloidal Suspensions of Nanometer-Sized Mesoporous Silica. *Adv Funct Mater* **2007**; 17: 605-12. <https://doi.org/10.1002/ADFM.200600578>
  28. Bilalis P, Tziveleka LA, Varlas S, Iatrou H. pH-Sensitive nanogates based on poly(L-histidine) for controlled drug release from mesoporous silica nanoparticles. *Polym Chem* **2016**; 7: 1475-85. <https://doi.org/10.1039/C5PY01841B>
  29. Zaharudin NS, Mohamed Isa ED, Ahmad H, Abdul Rahman MB, Jumbri K. Functionalized mesoporous silica nanoparticles templated by pyridinium ionic liquid for hydrophilic and hydrophobic drug release application. *Arab J Chem* **2020**; 24: 289-302. <https://doi.org/10.1016/J.JSCS.2020.01.003>
  30. Croissant J, Zhang D, Alsaïari S, Lu J, Deng L, Tamanoi F, et al. Protein-gold clusters-capped mesoporous silica nanoparticles for high drug loading, autonomous gemcitabine/doxorubicin co-delivery, and in-vivo tumor imaging. *J Control Release* **2016**; 229: 183-91. <https://doi.org/10.1016/J.JCONREL.2016.03.030>
  31. Möller K, Bein T. Talented mesoporous silica nanoparticles. *Chem Mater* **2017**; 29: 371-88. <https://doi.org/10.1021/ACS.CHEMMATER.6B03629>
  32. He H, Xiao H, Kuang H, Xie Z, Chen X, Jing X, et al. Synthesis of mesoporous silica nanoparticle-oxaliplatin conjugates for improved anticancer drug delivery. *Colloids Surf B Biointerfaces* **2014**; 117: 75-81. <https://doi.org/10.1016/J.COLSURFB.2014.02.014>
  33. Ortega E, Ruiz MA, Peralta S, Russo G, Morales ME. Improvement of mesoporous silica nanoparticles: A new approach in the administration of NSAIDs. *J Drug Deliv Sci Technol* **2020**; 58: 101833. <https://doi.org/10.1016/J.JDDST.2020.101833>
  34. Gandomkarzadeh M, Mahboubi A, Moghimi HR. Release behavior, mechanical properties, and antibacterial activity of ciprofloxacin-loaded acrylic bone cement: a mechanistic study. *Drug Dev Ind Pharm* **2020**; 46: 1209-18. <https://doi.org/10.1080/03639045.2020.1788058>
  35. Peppas NA, Buri PA. Surface, interfacial and molecular aspects of polymer bioadhesion on soft tissues. *J Control Release* **1985**; 2: 257-75. [https://doi.org/10.1016/0168-3659\(85\)90050-1](https://doi.org/10.1016/0168-3659(85)90050-1)
  36. GuhaSarkar S, Banerjee R. Intravesical drug delivery: Challenges, current status, opportunities and novel strategies. *J Control Release* **2010**; 148: 147-59. <https://doi.org/10.1016/J.JCONREL.2010.08.031>
  37. Kresge CT, Leonowicz ME, Roth WJ, Vartuli JC, Beck JS. Ordered mesoporous molecular sieves synthesized by a liquid-crystal template mechanism. *Nature* **1992**; 359: 710-2. <https://doi.org/10.1038/359710a0>
  38. Alswieleh AM, Alshahrani MM, Alzahrani KE, Alghamdi HS, Niazy AA, Alsilme AS, et al. Surface modification of pH-responsive poly(2-(tert-butylamino)ethyl methacrylate) brushes grafted on mesoporous silica nanoparticles. *Des Monomers Polym* **2019**; 22: 226-35. <https://doi.org/10.1080/15685551.2019.1699727>
  39. Cheng YJ, Zhang AQ, Hu JJ, He F, Zeng X, Zhang XZ. Multifunctional peptide-amphiphile end-capped mesoporous silica nanoparticles for tumor targeting drug delivery. *ACS Appl Mater Interfaces* **2017**; 9: 2093-103. <https://doi.org/10.1021/ACSAMI.6B12647>
  40. Solanki P, Patel A. Encapsulation of Aspirin into parent and functionalized MCM-41, in vitro release as well as kinetics. *Journal of Porous Materials* **2019**; 26: 1523-32. <https://doi.org/10.1007/S10934-019-00750-W>
  41. Xue JM, Shi M. PLGA/mesoporous silica hybrid structure for controlled drug release. *J Control Release* **2004**; 98: 209-17. <https://doi.org/10.1016/J.JCONREL.2004.04.023>
  42. Ludwig A. The use of mucoadhesive polymers in ocular drug delivery. *Adv Drug Deliv Rev* **2005**; 57: 1595-639. <https://doi.org/10.1016/J.ADDR.2005.07.005>
  43. Kim SN, Ko SA, Park CG, Lee SH, Huh BK, Park YH, et al. Amino-Functionalized Mesoporous Silica Particles for Ocular Delivery of Brimonidine. *Mol Pharm* **2018**; 15: 3143-52. <https://doi.org/10.1021/ACS.MOLPHARMACEUT.8B00215>